Available online at www.sciencedirect.com
SCIENCE DIRECT®
Journal of Inorganic Biochemistry 99 (2005) 45–54
Journal of Inorganic Biochemistry
www.elsevier.com/locate/jinorgbio

O_2-binding to heme: electronic structure and spectrum of oxyheme, studied by multiconfigurational methods

Kasper P. Jensen *, Björn O. Roos, Ulf Ryde

Department of Theoretical Chemistry, Chemical Centre, Lund University, P.O. Box 124, S-221 00 Lund, Sweden

Received 15 October 2004; received in revised form 20 October 2004; accepted 12 November 2004

Abstract

We have studied the ground state of a realistic model of oxyheme with multiconfigurational second-order perturbation theory (CASPT2). Our results show that the ground-state electronic structure is strongly multiconfigurational in character. Thus, the wavefunction is a mixture of many different configurations, of which the three most important ones are approximately $^1Fe^{II}$–$^1O_2$ (70%), Fe^{IV}–$^2O_2^{2-}$ (12%) and $^3Fe^{II}$–$^3O_2$ (3%). Thus, the wavefunction is dominated by closed-shell configurations, as suggested by Pauling, whereas the Weiss $^2Fe^{III} - ^2O_2^-$ configuration is not encountered among the 10 most important configurations. However, many other states are also important for this multiconfigurational wavefunction. Moreover, the traditional view is based on an oversimplified picture of the atomic-orbital contributions to the molecular orbitals. Thus, the population analysis indicates that all five iron orbitals are significantly occupied (by 0.5–2.0 electrons) and that the total occupation is most similar to the $^3Fe^{II}$–$^3O_2$ picture. The net charge on O_2 is small, -0.20 *e*. Thus, it is quite meaningless to discuss which is the best valence-bond description of this inherently multiconfigurational system. Finally, we have calculated the eleven lowest ligand-field excited states of oxyheme and assigned the experimental spectrum of oxyhemoglobin with an average error of 0.24 eV.

Keywords: Hemoglobin; O_2 binding; CASPT2; Density functional theory

1. Introduction

Hemes are an important and functionally diverse group of biological cofactors. Heme proteins are responsible for oxygen transport by globins, electron transfer by cytochromes, oxidation and hydroxylation reactions of vital importance in cytochromes P450, heme oxygenases and oxidoreductases, as well as scavenging of small oxidative-stress factors such as superoxide and peroxide by peroxidases and catalases [1].

A crucial feature of the iron protoporphyrin IX system is its ability to render all spin states of ferric and ferrous iron accessible [2], owing to the special design of the cavity in porphyrin, in contrast to other tetrapyrroles [3,4]. We have recently suggested that the axial ligands of heme proteins are tuned to bring spin states even closer in energy than they are in the free heme [5,6]. In particular, various choices of axial ligands or the tuning of their ligand field strength by proximal hydrogen bonds, for example [5], can be used to gather the spin states within a small energy range, thereby greatly facilitating binding of small ligands to the heme [6].

A classical example of such phenomenon is the binding of O_2 to deoxyheme, as it takes place in the globins: Deoxyheme is experimentally in the high-spin quintet state, whereas O_2 is a triplet and oxyheme is a singlet. Thus, the reactants involve a septet or triplet state (quintet + triplet), but the product is a singlet [7], which means that the reaction is formally spin forbidden [8]. Our results [6] indicate that nature has solved this problem by employing a heme group in which the quintet,

* Corresponding author. Tel.: +46 46 2224501; fax: +46 46 2224543.
E-mail address: Kasper.Jensen@teokem.lu.se (K.P. Jensen).

0162-0134/$ - see front matter © 2004 Published by Elsevier Inc.
doi:10.1016/j.jinorgbio.2004.11.008

triplet and singlet spin states are close in energy and for which the potential energy surfaces of the O_2 binding are very flat. Both these properties, together with the relatively high spin–orbit coupling of iron, strongly enhance the binding of O_2.

It is known that the heme–O_2 adduct contains dioxygen in a bent end-on binding mode [9]. However, the nature of the ground-state electronic structure remains an unsolved problem [10,11]. Three models, all satisfying the EPR silence (diamagnetic behavior) have been discussed. Pauling [7,12,13] suggested a closed-shell $^1Fe^{II}$–$^1O_2$ description with both moieties in the singlet state. On the other hand, Weiss [14] has argued that $^2Fe^{III}$–$^2O_2^-$ (doublet–doublet) provides a better explanation to the experimentally observed properties, i.e. that an electron is transferred from iron to O_2 upon binding. Finally, McClure [15] suggested a $^3Fe^{II}$–$^3O_2$ structure, with the O_2 molecule in its triplet ground state, but deoxyheme promoted from the high-spin ground state to the intermediate triplet-spin state. Subsequently, Goddard and Olafson [16,17] have expanded this idea into an ozone model, involving a three-center-four-electron bond. Other authors have stressed that several resonance forms may be necessary to properly describe the structure [10,18,19].

Many theoretical calculations have been performed on oxyheme models with the aim of settling the electronic structure, but with very varying results: Hartree–Fock calculations have been taken to support either the closed-shell Pauling picture [20] or the Weiss O_2^- model [21], whereas semi-empirical INDO calculations supported the Weiss model [22]. On the other hand, the result of another semi-empirical method (PPP) as well as density functional Xα calculations were interpreted as a mixture of the Pauling and ozone models [18,23] and this is also supported by multiconfigurational methods, which in general show a mixture of all the three models, but with the singlet Pauling model as the dominant configuration by 64–91% [24–26]. Yet, generalized valence bond calculations agreed with the ozone model [17] and the symmetry-adapted cluster configuration interaction (SAC-CI) method gave a Pauling-type ground state [27]. Finally, state-of-the-art density functional theory (DFT) calculations suggest an open-shell singlet ground state of oxyheme with spin polarization over the Fe–O bond [11,28,29]. Thus, they support the Weiss model as the best description of Fe–O_2 interaction or at least the dominant (2/3) configuration [6]. However, recent studies have repeatedly shown extensive differences between the predictions of DFT and more advanced coupled cluster and multiconfigurational methods [30,31].

The SAC-CI results were also used to study the vertical electronic excitation spectrum of oxyheme [24]. Unfortunately, the calculated spectrum was in poor agreement with the experimental results for the ligand-field spectrum [32] as well as the more intense porphyrin-based α, β and Soret bands [33] and only two bands were claimed to be reproduced out of seven ligand-field transitions and three porphyrin $\pi \rightarrow \pi^*$ transitions. For these two bands, assignment was different from the original one (which was based extended Hückel theory [32]) and the oscillator strengths differed by up to two orders of magnitude. Semiempirical PPP and DFT Xα methods have also been used to interpret the spectrum of oxyhemoglobin, but still with large errors in the calculated excitation energies (up to 1.68 eV) [30]. Recently, five ligand-field excitations in a O_2–porphyrin model were calculated by time-dependent DFT [34]. Three of them are close to the experimental results (0.01–0.10 eV), but no oscillator strengths were reported and the character of the excitations were not discussed.

This survey clearly shows that the electronic state of oxyheme and the interpretation of the electronic spectrum is far from settled. We present in this paper the most advanced calculation of the oxyheme electronic structure and ligand-field spectrum so far, based on multiconfigurational second-order perturbation theory. Our procedure takes into account both dynamical and non-dynamical correlation and all the relevant interactions in the ligand field, including Fe–O π effects, double-d-shell effects and porphyrin–iron σ interactions. The results provide a proper interpretation of the spectrum and show that the electronic state cannot be described by a single electronic configuration.

1.1. Methods

Our chemical model of oxyheme includes the porphine ring without any side chains, O_2 bound to iron and the imidazole group of the proximal histidine ligand [35]. The model is depicted in Fig. 1. The structure of the singlet ground state was optimized with the unrestricted BP86 DFT functional using the DZpdf basis set for iron [6] and 6–31G(d) for the other atoms. DFT has been readily applied to problems in porphyrin chemistry, providing excellent geometries of porphyrins in general [36,37]. The applied BP86 structure, which has been described before [6], is very close to experiment, as seen from Table 1. C_s symmetry with the O_2 molecule in a staggered position with respect to the equatorial Fe–N bonds was used because this is the optimum structure in the calculations, as well as in the experimentally observed state [6].

Calculations of the electronic spectrum were done with the Molcas 6.0 software [38], which includes the state-of-the-art implementation of CASPT2 (complete active space second-order perturbation theory) [39,40] for calculating accurate excitation energies using multiconfigurational wavefunctions [41]. We used the ANO-S basis set [42,43] with the contraction scheme [5s4p3d1f] for Fe, [3s2p1d] for N and O, [3s2p] for C

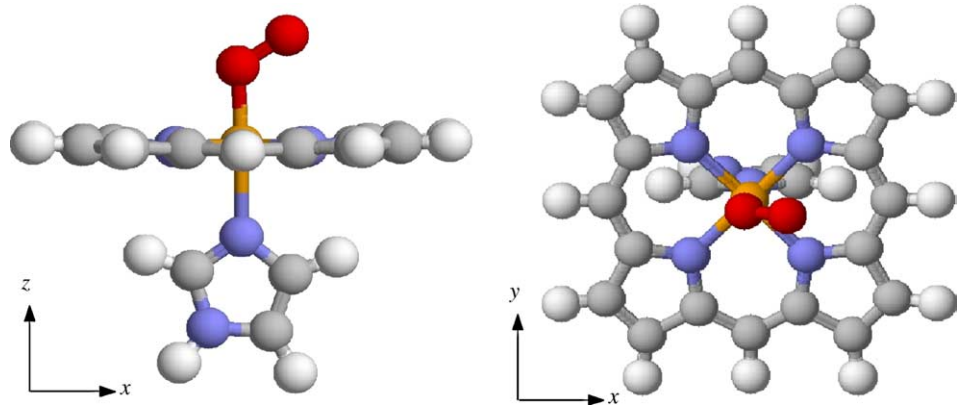

Fig. 1. The optimized oxyheme model of used in this work [6].

Table 1
Geometry of the model used in the calculations, compared to experiment

State	Fe–O	Fe–N_{ax}	Fe–N_{eq1}	Fe–N_{eq2}
$^1A'(1)$ [6]	1.807	2.096	2.024	2.001
Crystal [35]	1.806	2.064	2.006[a]	

[a] Average of the four Fe–N_{eq} distances.

and [2s] for H. This was the computationally largest possible basis set that still included a balanced treatment of correlation and polarization effects in the system.

The active space contained 14 electrons in 13 orbitals (7a + 6b) and it was designed to properly describe the ligand field of iron [44]. It is depicted in a partial density plot in Fig. 2. The shapes of the orbitals of the final active space are shown in Fig. 3 and their content is described in Table 2. To model correlation in the d shell

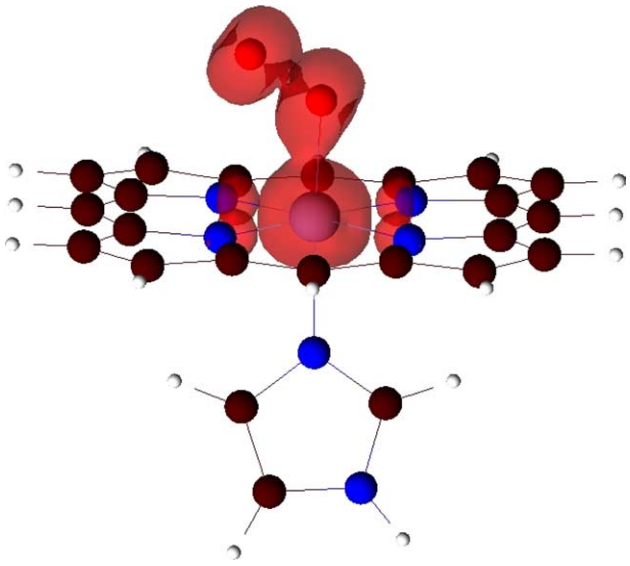

Fig. 2. The spatial extension of the active space, calculated from partial densities. The active-space density is depicted in red, with carbon atoms in black, hydrogens in white and nitrogen atoms in blue.

and to include the double-shell effect, all occupied Fe 3d orbitals (72a, 73a and 45b) were correlated by 4d orbitals (76a, 77a and 46b) and the bonding orbitals were described with antibonding correlating orbitals. Twelve of the active orbitals have significant Fe d character and five of them are almost pure d orbitals. Two orbitals are almost pure oxygen π orbitals (71a and 44b) and four contain both O_2 π* and Fe 3d character, important for describing the Fe–O bond (74a, 75a, 45b and 46b). An extra pair of orbitals from the porphine ring of b-symmetry was included, obtained as the highest occupied linear combination of the nitrogen σ orbitals, which is a four-center δ orbital interacting with the $d_{x^2-y^2}$ orbital of b-symmetry (43b, bonding and 47b, antibonding) in the final active space.

This active space satisfactorily describes the correlation effects in the ligand field and the Fe–O interaction and it includes the important double d shell and the Nσ orbital [44]. Therefore, it should give a give a good description of the electronic structure of the Fe–O adduct, as well as the ligand-field spectrum of the complex. However, it does not at all describe the electronic structure of the porphyrin and excitations within this ring. Yet, the results clearly shows that the porphine π system interacts very little with this ligand field. The HOMOs of the porphine are 70a and 42b, respectively (also shown in Fig. 3). Therefore, these orbitals do not need to be included in the active space, as was done in other CASPT2 studies of heme (which on the other hand did not included the important double d shell) [30,31].

The CASSCF (complete active space self-consistent field) wavefunction is used in CASPT2 as a reference to the second-order energy. This procedure is similar to Møller–Plesset second-order perturbation theory (MP2) using a CASSCF instead of a Hartree–Fock reference wavefunction. The CASSCF wavefunction captures the major part of the non-dynamical correlation energy by mixing configurations at the full CI level in the active space. Two state-average CASSCF calculations were performed, one including 6 roots of ^1A

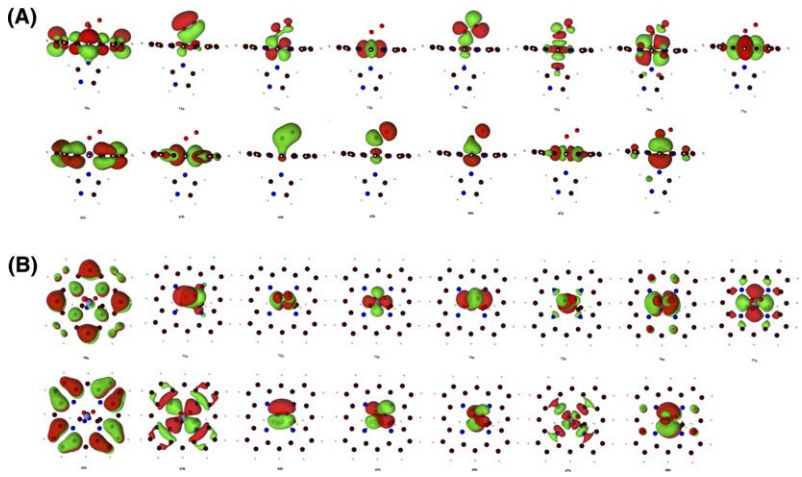

Fig. 3. The highest inactive (porphyrin π-type) and all active orbitals of symmetry a (top) and b (bottom). (A) side-view, (B) top-view. The colors correspond to positive (green) and negative (red) signs of the orbitals.

Table 2
Composition of active space CASSCF orbitals

MO	Type
71a	**O_2 π + Fe $3d_z^2$**
72a	**Fe $3d_{xz}$**
73a	**Fe $3d_{x^2-y^2}$**
74a	**O_2 π* + Fe $3d_{z^2}$**
75a	Fe $3d_{z^2}$ + O_2 π*
76a	Fe $4d_{xz}$
77a	Fe $4d_{x^2-y^2}$
43b	**Nσ + Fe $3d_{xy}$**
44b	**O_2 π**
45b	**O_2 π* + Fe $3d_{yz}$**
46b	Fe $3d_{yz}$ − O_2 π*
47b	Fe $3d_{xy}$ − Nσ
48b	Fe $4d_{yz}$

Orbitals in bold face are doubly occupied in the Hartree–Fock wavefunction.

symmetry and one with 6 roots of ^{1}B symmetry. All 1s orbitals and the 2s and 2p orbitals of Fe were frozen.

The second-order perturbation treatment was carried out using the multistate (MS) CASPT2 method [45], in which the space spanned by the state-average terms is subject to a perturbative Hamiltonian, where the diagonal elements correspond to the normal CASPT2 energies and the off-diagonal coupling elements represent the interaction under the influence of dynamic correlation. With diagonalization of this matrix, the MS-CASPT2 approach provides an adequate description in cases where the CASSCF wavefunction is not in itself a suitable reference, owing to strong coupling of the state-average CASSCF wavefunction, caused by dynamic correlation effects. The weight of the reference function for the excited states must be very close to that for the ground state, since the MS-CASPT2 approach is sensitive to the good convergence of the CASSCF wavefunction and to the absence of intruder states. The reference weights of all the perturbatively modified states were very similar (0.46–0.47), implying that our MS-CASPT2 description is valid. We applied a level shift of 0.3 to reduce the influence of intruder states. This is known not to affect the accuracy of CASPT2, which is ~0.3 eV for excitation energies when a saturated active space and a reasonable basis set is applied [46].

Throughout the article, we use a coordinate system in which Fe is at the origin, the oxygen atom that binds to Fe is on the positive *z*-axis and dioxygen as well as imidazole are in the *xz*-symmetry plane, which intersects the pyrrole nitrogen atoms (cf. Fig. 1).

2. Results and discussion

2.1. Nature of the ground state

The obtained ground state, ^{1}A(1), is a mixture of a large number of different configurations. The 10 configuration state functions (CSF) with the highest weights are presented in Table 3 (with a cumulative weight of 91%). The most important configuration (weight 70%) has two electrons in MOs 71a–74a and 43b, 44b and 46b. If we use the interpretation of the active MOs in Table 2 and assign orbitals 74a and 45b as the two O_2 π* orbital and orbitals 72a, 73a, 75a, 46b and 47b as the five Fe 3d orbitals (this assignment is of course approximate because the orbitals are in reality delocalized, as can be seen in Fig. 3), then we can conclude that this configuration is essentially the closed-shell Pauling structure, $(d_{xz})^2(d_{x^2-y^2})^2(d_{yz})^2(\pi_a^*)^2$. However, it should be noted that although the d_{xz} and $d_{x^2-y^2}$ orbitals (72a and 73a) are rather pure, MO 46b is a strong mixture of d_{yz} and the O_2 π* orbital, with only a small excess of the former (Fig. 3). Likewise, MO 43b has significant amount of d_{xy}, forming an antibonding interaction with the pyrroles.

Table 3
The 10 most important configuration state functions (CSF) of the ground-state wave function

#	CSF[a]	Weight (%)
1	2222000 220200	69.8
2	2222000 222000	11.9
3	222ud00 22ud00	3.2
4	2222000 202200	1.1
5	222ud00 2ud200	0.9
6	2220200 220200	0.9
7	2220200 222000	0.8
8	222uu00 22dd00	0.6
9	222ud00 2u2d00	0.6
10	u222d00 2ud200	0.5

[a] See Table 2 for the numbering of the active orbitals (7 in symmetry a, 6 in b). "2" means a doubly occupied orbital, "u" singly occupied with spin up, "d" singly occupied with spin down and "0" an unoccupied orbital. The CSFs are eigenfunctions of the spin operators.

The second configuration (weight 12%) is made up of the closed-shell double excitation of MO 46b to 45b. In our interpretation, this is $(d_{xz})^2(d_{x^2-y^2})^2(\pi_a^*)^2(\pi_b^*)^2$, i.e. formally $^1Fe^{IV}-{}^1O_2^{2-}$. This model has frequently been suggested as an alternative resonance state of the closed-shell Pauling structure [13,19].

The third important configuration (weight 3%) involves two excitations: In the first, an electron is excited from MO 46b to 45b, i.e. between the two orbitals that are a mixture of d_{yz} and the O_2 π^*. The second is the 74a → 75a excitation, which is also an excitation between two orbitals that are a mixture of Fe 3d (d_z^2) and O_2 π^*. Even if both excitations formally are of charge-transfer type, little charge is actually transferred, owing to the similarity of the two MOs involved. The resulting state is formally $(d_{xz})^2(d_{x^2-y^2})^2(d_{yz})^1(d_{z^2})^1(\pi_a^*)^1(\pi_b^*)^1$, which actually is the triplet–triplet coupled McClure or ozone model.

The remaining states all have a weight of ⩽1%. Three of them are closed-shell configurations. Number 4 (weight 1%) involves a double $\pi \rightarrow \pi^*$ excitation. Number 6 and 7 are alternative Pauling structures with the interpretations $(d_{xz})^2(d_{x^2-y^2})^2(d_{z^2})^2(d_{yz})^2$ and $(d_{xz})^2(d_{x^2-y^2})^2(d_{z^2})^2(\pi_b^*)^2$, i.e. a $^1Fe^0-{}^1O_2^{2+}$ and the standard Pauling $^1Fe^{2+}-{}^1O_2$ state, but with only Fe 3d orbitals of a symmetry and with the π_b^* orbital occupied.

State 8 (0.6%) is notable because it has the same occupation as in the ozone state (number 3), but with an internal coupling of the electrons on iron and on O_2. The remaining three states involve two excitations, including at least one from the bonding O_2 π orbitals and they thus describe static correlation in the O–O bond.

It is notable that the Weiss configuration ($Fe^{III}-O_2^-$, i.e. 2222000 22ud00 with the formalism in Table 3) is not encountered among the important configurations. In fact, there are four states with two singly occupied orbitals among the 20 most important configurations (with a total weight of 1.4%), but they all involve additional excitations, e.g. 45b → 44b in state 11 (i.e. formally $^2Fe^I-{}^2O_2^+$).

This picture of the nature of the electronic ground state can be supplemented by the occupation numbers of the active natural orbitals, which are 1.98, 1.96, 1.97, 1.87, 0.16, 0.02, 0.02 for the a orbitals (71a–77a) and 1.98, 1.93, 0.44, 1.63, 0.04 and 0.01 for the b orbitals (43b–48b). Again, we see that the Pauling configuration dominates, although MO 45b (mainly O_2 π^*) is almost half occupied and MO 75a (Fe $3d_z^2$) is also significantly occupied (0.2).

An alternative way to analyze the electronic character of the ground-state wavefunction is to look at the Mulliken populations of the various atoms and atomic orbitals. These are given in Table 4. From these, it can directly be seen that the charge of the O_2 moiety is −0.20 *e*, which shows that only little charge is transferred from iron to O_2. This shows that the Weiss description ($Fe^{III}-O_2^-$) is of less importance for the ground state of oxyheme. As a comparison, it can be mentioned that DFT, in which the Weiss state is the major configuration of the system, the Mulliken charge of O_2 is more negative (−0.32 to −0.42 *e* depending on the functional used) [6], but still far from −1, expected for a pure O_2^- state.

The Mulliken charge on the iron ion is 0.93 *e*, which shows that much of the formal +2 charge has been transferred to the imidazole ligand and the porphyrin ring. The total 3d population is 6.37 *e*. This is actually higher than what is expected for any of the three models of the oxyheme ground state (6 or 5 *e*). On the other hand, it is similar to the population of the same model without the O_2 molecule, calculated in the high-spin state with the corresponding active space (8 electrons in 9 orbitals), 6.23 *e*. This shows that there has not been any appreciable transfer of charge, again speaking against the Weiss description. The individual Fe 3d populations are 1.97, 1.95, 1.28, 0.68 and 0.49 *e*. This is

Table 4
Mulliken orbital populations for Fe 3d and O 2p orbitals

Fe (total 6.37)					O1 (total 4.16)			O2 (total 4.11)		
$3d_{x^2-y^2}$	$3d_{xz}$	$3d_{yz}$	$3d_z^2$	$3d_{xy}$	$2p_x$	$2p_y$	$2p_z$	$2p_x$	$2p_y$	$2p_z$
1.97	1.95	1.28	0.68	0.49	1.27	1.49	1.40	1.27	1.20	1.64

O1 is the oxygen atom that coordinates directly to Fe.

closer to what is expected for the ozone description (2, 2, 1, 1, 0) than to the Pauling (2, 2, 2, 0, 0) or the Weiss (2, 2, 1, 0, 0) descriptions, but it clearly shows that all three models are oversimplifications of the true multiconfigurational ground state.

It is clear that the present calculations indicate that the Pauling structure is the dominant contribution to the ground-state wavefunction of oxyheme. However, the weight of this state is only 70% (85% if all the closed-shell configurations in Table 3 are included). Thus, only part of the wavefunction can be explained with this model. This is also supported by the 0.44 occupation number of the alternative MO 45b. Moreover, this interpretation is based on a very simplistic identification of the dominant atomic-orbital component of the mixed molecular orbitals. In fact, the Mulliken population analysis indicates that the wavefunction actually is better described by the ozone model than by the Pauling model. Similar results were obtained in the previous, less accurate, CASSCF calculations by Yamamoto and Kashiwagi [26] (with 14 electrons in 11 active orbitals, including only one Fe 3d shell); they obtained a similar weight of the dominant Pauling configuration 68%, although they obtained occupation numbers of the $3d_{yz}$ and $3d_{z^2}$ orbitals closer to one (1.08 and 0.97). These calculations have in common that they give little support of the Weiss model, which is the dominant contribution in DFT calculations.

Thus, we can conclude that oxyheme is strongly multiconfigurational. This explains why earlier investigations have given so varying results. The multiconfigurational character of the wavefunction can only be accurately described by multireference methods like CASSCF. It is also hard to describe the total wavefunction in simple and intuitive terms as atomic orbitals, resonance structures, or valence bond pictures, as also has been discussed before [19]. Thus, it is quite meaningless to discuss which of the three models is the best description of oxyheme because the correct answer is that it is a mixture of many different configurations.

A check of the quality of the calculated wavefunction is to estimate quadrupole splitting parameters (ΔE_Q) from the electric field gradients with standard methods [47] and compare with experimental data from Mössbauer experiments. From the CASSCF wavefunction, we get a ΔE_Q value of −1.87 mm/s, oriented in the x-direction and an asymmetry parameter (η) of 0.13. This is quite close to experimental data for model compounds, −2.10 mm/s and 0.23 in x- or y-direction [48], as well as for oxymyoglobin (−2.3 mm/s) [49] and oxyhemoglobin (−2.24 mm/s) [50]. In particular, it is appreciably closer than earlier CASSCF estimates: −0.98 mm/s and 0.72 [26]. DFT with the same method as the geometry optimization also gives similar results: −2.52 mm/s and 0.24.

Table 5
Experimental assignment of the ligand-field spectrum of oxyhemoglobin

State	Energy (eV)	Experimental assignment
I	0.95	$d_{xz} + O_2\ \pi_g^* \rightarrow d_{yz} + O_2\ \pi_g^*$
II	1.08	$d_{x^2-y^2} \rightarrow d_{yz} + O_2\ \pi_g^*$
III	1.26	$a_{2u}(\pi) \rightarrow d_{yz} + O_2\ \pi_g^*$
IV	1.59	$a_{1u}(\pi) \rightarrow d_{yz} + O_2\ \pi_g^*$
V	2.28	$d \rightarrow d$
VI	2.73	$d \rightarrow d$
VII	3.84	$O_2\pi_u^* \rightarrow d_{yz} + O_2\pi_g^*$

Reference [32]. Note that we use a slightly different coordinate system that in the original publication (the x and y axes have been interchanged).

2.2. The ligand-field spectrum

The experimental ligand-field absorption spectrum of oxyhemoglobin has been studied by Eaton et al. [29]. The near-infrared part of the spectrum was assigned with seven bands (I–VII) based on extended Hückel calculations, as is shown in Table 5. All assignments were excitations to a combination of Fe $3d_{yz}$ and O_2 π_g or to unspecified d orbitals. Two of the bands (III and IV) were supposed to be porphyrin-to-metal charge-transfer excitations. Bands II, V and VI were assigned as excitations from Fe 3d orbitals. Band I was assigned as a $d_{xz} \rightarrow d_{yz}$ excitation, whereas band VII was assigned as partial excitation from a O_2 antibonding π_u orbital to d_{yz}.

Table 6 shows the energies and composition of the excited states, whereas Table 7 describes the computed spectrum and compares it to the experimental spectrum. Seven lines appear in the experimental spectrum, but band VII is at a higher energy than we have studied. We have tried to use a larger number of CI roots, but this destroyed the active space and gave erroneous results for some states. We have assigned our states based on their oscillator strengths. Seven computed states have oscillator strengths $>10^{-6}$ and six of them can be directly assigned. The largest error in this assignment is 0.4 eV, with an average absolute error of 0.24 eV. Two of the assigned states are of b symmetry, the four others of a symmetry. Two states, ^{1}A(3) and ^{1}B(2), have errors slightly larger than what could be expected from CASPT2: 0.35 and 0.40 eV, respectively. The rest fall within the expected uncertainty of the method (~0.3 eV). Characteristic for the spectrum is that most of the excited states have large contributions from doubly excited configurations.

When analyzing the electronic transitions it is important to note that such an analysis depends strongly on the choice of orbitals. The same total wavefunction can be represented by different sets of orbitals. This is true for Hartree–Fock as well as CASSCF wavefunctions. It is possible to rotate the inactive and active orbitals into each other without changing any of the

Table 6
Energies (eV) and composition of low-lying states obtained with various methods

State	CAS	PT2	MS	Primary configuration	Second configuration	Third configuration
^{1}A(1)	0.00	0.00	0.00	2222000 220200	2222000 22ud00	222ud00 22ud00
^{1}A(2)	1.85	1.29	1.31	2222000 220200	2222000 22ud00	2u2d000 222200
^{1}A(3)	2.14	1.96	1.94	2u2d000 222200	22ud000 222200	2222000 220200
^{1}A(4)	2.46	2.16	2.07	22ud000 222200	2u2d000 222200	22ud000 22u2d0
^{1}A(5)	2.57	2.03	2.23	22ud000 22u2d0	22uu000 22d2d0	22ud000 222200
^{1}A(6)	2.90	2.92	3.00	2220000 222200	u22d000 222200	0222000 222200
^{1}B(1)	0.76	0.30	0.30	2u22000 2220d0	2u22000 22d020	2ud2u00 2220d0
^{1}B(2)	0.98	1.12	0.55	222u000 2220d0	222u000 22d020	22udu00 2220d0
^{1}B(3)	1.12	0.58	0.76	22u2000 22d020	22u2000 22dud0	22u2000 222d00
^{1}B(4)	2.54	1.88	1.29	22u2000 2220d0	222u000 222d00	22u2000 22dud0
^{1}B(5)	2.80	0.84	1.91	222u000 222d00	222u000 220d20	22u2000 222d00
^{1}B(6)	2.87	2.03	2.15	22u2000 22d020	22u2000 2220d0	22u2000 22dud0

CAS, CASSCF; PT2, CASPT2; MS, MS-CASPT2. See Table 4 for an explanation of the labeling scheme of the configurations.

properties of the wave function. But the CAS-CI expansion coefficients will change. Any discussion of the electronic structure, which is based on orbitals is therefore in a way arbitrary.

The calculations of the excited states use state-average orbitals for the six lowest states in symmetry ^{1}A (and a different set for the six states of symmetry ^{1}B). These orbitals are different from the orbitals obtained in a calculation of only the ground state. It should also be borne in mind that the analysis of the excitation pattern will be different when using state average orbitals than it would have been using ground state orbitals. Nevertheless we attempt below an interpretation of the excitations in terms of the orbitals used in the calculation. In the state-average calculation, the ground state contains only 44% of the Pauling configuration, 10% of the ozone configuration and 6% $^2Fe^{IV} - {}^2O_2^{2-}$ (Table 6). Moreover, it contains 18% of the Weiss configuration, which was not seen at all in the CASSCF calculation optimized only for the ground state.

Starting with the symmetric states, the ^{1}A(2) state is assigned to band III as the only intense line close to 1.26 eV (1.31 eV). This state has a similar amount of the Weiss configuration as the ground state (18%) but contains less of the Pauling configuration (20%). The McClure configuration is insignificant in this state. Instead, a partial 74a → 75a single excitation and the 74a → 45b and 72/74a → 45b double excitations account for the state. These excitations can be described as ligand-to-metal charge-transfer (LMCT) FeO, O_2 $\pi_a^* \rightarrow \pi_b^*$ and MLCT FeO. The extended Hückel assignments of porphyrin-to-metal charge transfer bands are incorrect, since our results clearly show that there is no communication between the ligand and the metal: We have not observed any intruder states with ligand character.

Table 7
Calculated and experimental ligand-field absorption spectrum. The excitations are denoted (S) for single excitations and (D) for double excitations

State	MS-CASPT2			Experiment [32]			#	Our assignment (main excitations)
	E	λ	*f*	*E*	λ	*f*		
^{1}A(2)	1.31	944	0.005660	1.26	980	0.00260	III	74a → 75a (S) 74a → 45b (D) 72/74a → 45b (D)
^{1}A(3)	1.94	641	0.000494	1.59	781	0.00210	IV	72/74a → 45b (D) 73/74a → 45b (D)
^{1}A(4)	2.07	598	0.000001					
^{1}A(5)	2.23	555	0.000121	2.28	544	N.A.	V	73/74a → 45/47b (D)
^{1}A(6)	3.00	413	0.000919	2.73	455	0.02200	VI	74a → 45b (D) 71/74a → 45b (D) 71a → 45b (D)
^{1}B(1)	0.30	4161	1.89E-07					
^{1}B(2)	0.55	2253	0.000025	0.95	1299	0.00005	I	74a → 47b (S) 74a/45b → 47b (D) 73/74a → 75a/47b (D)
^{1}B(3)	0.76	1627	0.000001	1.08	1149	0.00030	II	73a,45b → 47b (D)
^{1}B(4)	1.29	963	4.27E-08					
^{1}B(5)	1.91	649	1.77E-07					
^{1}B(6)	2.15	576	1.05E-07					

Energies (*E*) are in eV, wavelengths (λ) in nm and oscillator strengths (*f*) in atomic units.

The next state, ^{1}A(3) at 1.94 eV, is assigned to band IV (1.59 eV). The agreement is not so good for this state. It contains a mixture of various double excitations and is described mainly by the same 72/74a → 45b double excitation as before (MLCT FeO and O_2 $\pi^*_a \rightarrow \pi^*_b$), together with a similar 73/74a → 45b double excitation, from $d_{x^2-y^2}$ instead of from d_{xz}. This state is thus a strong MLCT state and this may be the reason why it is less well predicted than the other states in the spectrum.

We then turn to ^{1}A(5) at 2.23 eV, which we assign to band V (2.28 eV). It consists mainly (53%) of the configuration state function 22ud000 22u2d0, which corresponds to double excitations from $3d_{x^2-y^2}$ and O_2 π^*_a to O_2 π^*_b and $3d_{yz}$. The second most important configuration is the O_2 $\pi^*_a \rightarrow \pi^*_b$ double excitation, 74a → 45b. Thus, this is not a charge-transfer state.

The ^{1}A(6) state at 3.00 eV is assigned as band VI (2.73 eV). It can be described as a O_2 $\pi^* \rightarrow \pi^*$ excited state, with two double excitations, 71/74a → 45b and 71a → 45b as the most important contributions.

The ^{1}B states generally have small oscillator strengths, but two of them are strong enough to be observed experimentally. ^{1}B(2) at 0.55 eV is assigned to band I with an experimental excitation energy of 0.95 eV. It consists of three major excitations: a singlet 74a → 47b LMCT excitation from mainly O_2 π^* to the antibonding Fe $3d_{xy}$–Nσ orbital in the porphyrin plane, a double 74a/45b → 47b LMCT excitation and a 73a/74a → 75a/45b double excitation. This is a strong LMCT state, which may be the reason why it together with ^{1}A(3) is slightly less accurately modeled than the other states.

Finally, the ^{1}B(3) state at 0.76 eV is assigned to band II at 1.08 eV. It also has LMCT nature, owing to the dominant 73a/45b → 47b excitation. This configuration corresponds to exciting one electron from Fe $3d_{x^2-y^2}$ and another from the mainly O_2 π^* MO, both to the antibonding Fe $3d_{xy}$–Nσ orbital in the porphyrin plane.

Altogether, the experimental spectrum is assigned with intense peaks well accounted for, except for band VII, which is out of range of our computation. The three largest errors in our excitation energies, 0.32–0.40 eV, are slightly larger than expected for CASPT2 on organic molecules. These errors are caused by the strong charge-transfer character of these states, as was discussed above. The remaining excited states have a mean absolute error of only 0.12 eV. Considering that the experimental spectrum is done on hemoglobin in solution and our model includes only iron, imidazole, O_2 and porphine, this is surprisingly good and better than earlier theoretical attempts on this spectrum [27,32].

As was mentioned in the introduction, the ligand-field spectrum of the oxyheme model in Fig. 1 has also been studied by time-dependent DFT with ligand-field excitations at 0.41, 0.85, 1.09, 1.18 and 1.27 eV [34]. Since no details are given for these calculations, we have repeated them with our geometry (with the same method and basis sets as in the geometry optimisation). We obtain bands at 0.40, 0.56, 0.72, 1.24 (all of b symmetry) and 1.37 eV (a symmetry). Above ~1.2 eV, a quite dense spectrum is encountered with mainly porphyrin excitations (80 bands below 3.3 eV). Thus, the DFT spectrum is very close to the CASPT2 spectrum with an average difference of 0.05 eV, which was quite unexpected, considering that many of the lines involve double excitations.

Finally, we have also calculated the energy of the lowest triplet and quintet states with CASPT2. The results indicate that the ^{3}A, ^{5}A and ^{5}B states are 0.67, 0.41, 0.37 eV above the ^{1}A ground state. However, the ^{3}B state actually comes out 0.12 eV below the ^{1}A ground state. Of course, this is contrary to the experimental observation of a singlet ground state of oxyheme, but the energy difference is smaller than the expected accuracy of the CASPT2 method, ~0.3 eV. Thus, our results support the observation by DFT that there are triplet and quitet states within 0.3 eV of the singlet ground state, states which may facilitate the formally spin-forbidden binding of O_2 [6]. On the other hand, the accuracy of our method gives no opportunity to decide whether or not there is a very low-lying (thermally populated) triplet state, as has been suggested for oxyhemoglobin (0.018 eV) [51]. The latter results have been questioned on experimental grounds [52]. Previous calculations have given higher energies of the triplet state (0.11–1.2 eV) [16,18,24,27], although the INDO-CI method supported a thermally populated triplet state (0.019 eV) [22].

3. Conclusions

We have studied the ground state and the first eleven excited electronic ligand-field states of oxyheme with multiconfigurational second-order perturbation theory. Considering the extensive multiconfigurational character of the ground state of the Fe–O_2 interaction, this should be the only type of methods that gives an accurate and balanced description of the ground state (although DFT undoubtedly provides an excellent geometry of the oxyheme model [6], cf. Table 1, and also a reasonably accurate description of the electronic spectrum).

Two groups have used similar methods before to study this system, viz. Newton and Hall with the generalized molecular orbital + CI method (essentially a multireference CI method) [24] and Yamamoto and Kashiwagi with CASSCF calculations [25,26]. However, these investigations are 10–20 years old. Today's methods and software allow for much more accurate calculations with more realistic models, larger basis sets

and larger active spaces. As a consequence, the present calculations give a different picture than the older studies.

The main conclusion of this work regards the ground state electronic structure of oxyheme. Whereas Pauling emphasized a $^{1}Fe^{II}$–$^{1}O_2$ description [7,12,13], McClure, as well as Olafson and Goddard, a $^{3}Fe^{II}$–$^{3}O_2$ (ozone) description [15–17] and Weiss a $^{2}Fe^{III} - {}^{2}O_2^{-}$ description [14], we have shown here that our calculated wavefunction is a mixture of many different configurations. In fact, various ways to interpret the wavefunction give different weights of the configurations, owing to the problem of interpreting a complex multiconfigurational wavefunction in simple atomic-orbital terms.

Even if it is clear that a multiconfigurational description of oxyheme is necessary, it is not certain that any CASSCF calculation will give an accurate description of the electronic ground state. On the contrary, the results of CASSCF calculations strongly depends on the choice of the active-space orbitals [44]. Experience has taught us that the active space must be selected to accurately describe the site of interest, especially considering the quite restrictive upper limits of the active space ($\sim$14 orbitals) [38]. The present active space has been carefully selected to describe in particular the Fe ligand field and the Fe–O_2 interaction. Thus, all five Fe 3d orbitals were included, as well as correlating orbitals to all the occupied 3d orbitals. Likewise, all four O_2 π and π^* orbitals were included in the active space. The appropriateness of this space is illustrated by the quality of the calculated ligand-field and O_2 charge-transfer excitation energies and by the absence of intruder states.

Therefore, we are quite convinced that the present description of the oxyheme electronic ground state is accurate and will not change considerably if the calculations are improved by larger active spaces or better basis sets. We can conclude that the electronic structure of oxyheme is a strong multiconfigurational mixture of many different valence-bond states. However, it is dominated by a description involving only doubly occupied orbitals.

Acknowledgments

This investigation has been supported by grants from the Swedish Research Council and by Computer Resources of Lunarc at Lund University.

References

[1] M. Sono, M.P. Roach, E.D. Coulter, J.H. Dawson, Chem. Rev. 96 (1996) 2841–2888.
[2] W.R. Scheidt, C.A. Reed, Chem. Rev. 81 (1981) 543–555.
[3] K.P. Jensen, U. Ryde, ChemBioChem 4 (2003) 413–424.
[4] K.P. Jensen, U. Ryde, J. Phys. Chem. B, submitted.
[5] K.P. Jensen, U. Ryde, Mol. Phys. 101 (2003) 2003–2018.
[6] K.P. Jensen, U. Ryde, J. Biol. Chem. 279 (2004) 14561–14569.
[7] L. Pauling, C.D. Coryell, Proc. Natl. Acad. Sci. USA 22 (1936) 210–216.
[8] M. Kotani, Rev. Mod. Phys. 35 (1963) 717–720.
[9] A.K. Churg, M.W. Makinen, J. Chem. Phys. 68 (1978) 1913–1925.
[10] I. Bytheway, M.B. Hall, Chem. Rev. 94 (1994) 639–658.
[11] M. Kaupp, C. Rovira, M. Parinello, J. Phys. Chem. B 104 (2000) 5200–5208.
[12] L. Pauling, Stanford Med. Bull. 6 (1948) 215–217.
[13] L. Pauling, Nature 203 (1964) 182–183.
[14] J.J. Weiss, Nature 202 (1964) 83–84.
[15] D.S. McClure, Radiat. Res. Suppl. 2 (1960) 218–242.
[16] W.A. Goddard, B.D. Olafson, Proc. Natl. Acad. Sci. USA 72 (1975) 2335–2339.
[17] B.D. Olafson, W.A. Goddard, Proc. Natl. Acad. Sci. USA 74 (1977) 1315–1319.
[18] B.H. Huynh, D.A. Case, M. Karplus, J. Am. Chem. Soc. 99 (1977) 6103–6105.
[19] D.A. Summerville, R.D. Jones, B.M. Hoffman, F. Basolo, J. Chem. Educ. 56 (1979) 157–162.
[20] A. Dedieu, M.-M. Rohmer, M. Benard, A. Veillard, J. Am. Chem. Soc. 98 (1976) 3717–3718.
[21] T. Nozawa, M. Hatano, U. Nagashima, S. Obara, H. Kashiwagi, Bull. Chem. Soc. Jpn. 56 (1983) 1721–1727.
[22] Z.S. Herman, G.H. Loew, J. Am. Chem. Soc. 102 (1980) 1815–1821.
[23] D.A. Case, B.H. Huynh, M. Karplus, J. Am. Chem. Soc. 101 (1979) 4433–4453.
[24] J.E. Newton, M.B. Hall, Inorg. Chem. 23 (1984) 4627–4632.
[25] S. Yamamoto, H. Kashiwagi, Chem. Phys. Lett. 161 (1989) 85–89.
[26] S. Yamamoto, H. Kashiwagi, Chem. Phys. Lett. 205 (1989) 306–312.
[27] H. Nakatsuji, J. Hasegawa, M. Hada, Chem. Phys. Lett. 250 (1996) 379–386.
[28] C. Rovira, K. Kunc, J. Hutter, P. Ballone, M. Parrinello, J. Phys. Chem. A 101 (1997) 8914–8925.
[29] E. Sigfridsson, U. Ryde, J. Biol. Inorg. Chem. 4 (1999) 99–110.
[30] A. Ghosh, B.J. Persson, P.R. Taylor, J. Biol. Inorg. Chem. 8 (2003) 507–511.
[31] A. Ghosh, P.R. Taylor, Curr. Opin. Chem. Biol. 7 (2003) 113–124.
[32] W.A. Eaton, L.K. Hanson, P.J. Stephens, J.C. Sutherland, J.B.R. Dunn, J. Am. Chem. Soc. 100 (1978) 4991–5003.
[33] M. Nagai, Y. Sugita, Y. Yoneyama, J. Biol. Chem. 247 (1972) 285–290.
[34] F. De Angelis, R. Car, T.G. Spiro, J. Am. Chem. Soc. 125 (2003) 15710–15711.
[35] J. Vojtechovsky, K. Chu, J. Berendzen, R.M. Sweet, I. Schlichting, Biophys. J. 77 (1999) 2153–2174.
[36] A. Ghosh, Acc. Chem. Res. 31 (1998) 189–198.
[37] A. Ghosh, E. Steene, J. Biol. Inorg. Chem. 6 (2001) 739–752.
[38] G. Karlström, R. Lindh, P.-Å. Malmqvist, B.O. Roos, U. Ryde, V. Veryazov, P.-O. Widmark, M. Cossi, B. Schimmelpfennig, P. Neogrady, L. Seijo, Computational Material Science 28 (2003) 222–239.
[39] K. Andersson, P.-A. Malmqvist, B.O. Roos, A.J. Sadlej, K. Wolinski, J. Phys. Chem. 94 (1990) 5483–5488.
[40] K. Andersson, P.-A. Malmqvist, B.O. Roos, J. Chem. Phys. 96 (1992) 1218–1226.
[41] B.O. Roos, K. Andersson, M.P. Fülscher, P.-Å. Malmqvist, L. Serrano-Andrés, K. Pierloot, M. Merchán, in: I. Prigogine, S.A. Rice (Eds.), Advances in Chemical Physics: New Methods in Computational Quantum Mechanics, XCIII, Wiley, New York, 1996, pp. 219–331.

[42] P.-O. Widmark, P.-Å. Malmqvist, B.O. Roos, Theor. Chim. Acta 77 (1990) 291–306.
[43] P.-O. Widmark, J.B. Persson, B.O. Roos, Theor. Chim. Acta 79 (1991) 419–432.
[44] K. Pierloot, Mol. Phys. 101 (2003) 2083–2094.
[45] J. Finley, P.-Å. Malmqvist, B.O. Roos, L. Serrano-Andrés, Chem. Phys. Lett. 288 (1997) 299–306.
[46] B.O. Roos, K. Andersson, M.P. Fülscher, L. Serrano-Andrés, K. Pierloot, M. Merchán, V. Molina, J. Mol. Struct.: THEOCHEM 388 (1996) 257–276.
[47] S. Yamamoto, J. Teraoka, H. Kashiwagi, J. Chem. Phys. 88 (1988) 303–310.
[48] K. Spartalian, G. Lang, J.P. Colman, R.R. Gagne, C.A. Read, J. Chem. Phys. 63 (1975) 5375–5382.
[49] B. Boso, P.G. Debrunner, G.C. Wagner, T. Inubushi, Biochim. Biophys. Acta 701 (1984) 244–251.
[50] G. Lang, W. Marshall, J. Mol. Biol. 18 (1966) 385–389.
[51] M. Cerdonio, A. Congiu-Castellano, F. Mogno, B. Pispisa, G.L. Romani, S. Vitale, Proc. Natl. Acad. Sci. USA 74 (1977) 398–400.
[52] L. Pauling, Proc. Natl. Acad. Sci. USA 74 (1977) 2612–2613.

Available online at www.sciencedirect.com
SCIENCE DIRECT®
Journal of Inorganic Biochemistry 99 (2005) 978
Journal of Inorganic Biochemistry
www.elsevier.com/locate/jinorgbio

Erratum

Erratum to "O_2-binding to heme: electronic structure and spectrum of oxyheme, studied by multiconfigurational methods" [J. Inorg. Biochem. 99(1) (2004) 45–54]

Kasper P. Jensen, Björn O. Roos, Ulf Ryde *

Department of Theoretical Chemistry, Lund University, Chemical Centre, P. O. Box 124, S-221 00 Lund, Sweden

Received 12 January 2005; received in revised form 11 February 2005; accepted 14 February 2005
Available online 9 March 2005

Keywords: Hemoglobin; O_2 binding; CASPT2; Density functional theory

In the paper "O_2-binding to heme: electronic structure and spectrum of oxyheme, studied by multiconfigurational methods" published in the first volume of this series [1], there was a misinterpretation of the structure of the electronic wavefunction for the ground state of the oxyheme molecule, which led to wrong conclusions concerning the type of bond formed between iron and the oxygen molecule. Here, we give the correct interpretation, which should complement the discussion in section 2.1 in [1].

The most important part of the CASSCF multiconfigurational wavefunction for the ground state of oxyheme can be written as a linear combination of three terms

$$\Psi = 0.835(74a)^2(46b)^2 - 0.345(74a)^2(45b)^2 - 0.179(74a)^1(75a)^1(45b)^1(46b)^1 + \cdots, \quad (1)$$

where all orbital labels refer to those in [1] and the orbitals are shown in Fig. 3 in [1]. Only orbitals with differing occupation numbers have been included in Eq. (1). The two first terms are the most important for the discussion. It was correctly stated in [1] that the first term corresponds to the closed-shell Pauling configuration. But the weight of this configuration is not one, but only 70% (0.835^2). Orbitals 74*a* and 46*b* are σ and π bonding between Fe and O, respectively. The next configuration has orbital 46*b* replaced by the corresponding π antibonding orbital 45*b*. It has a weight of 12%. Suppose that the weight of these two configurations were equal. We could then have made a transformation to localized orbitals, π^* on O_2 and $3d_{yz}$ on iron. The two configurations would in this representation have collapsed into one: $(\pi^*)^1(3d_{yz})^1$, where the two electrons are coupled to a singlet. This is the Weiss configuration. Thus, we can conclude that the wavefunction in Eq. (1) is a mixture of the Pauling and Weiss configurations. The two configurations overlap, so it is not possible to give a precise measure of their relative importance, but an estimate indicates that they are of similar weight. The conclusion is thus that the CASSCF wavefunction for the ground state of oxyheme is dominated by the Pauling and Weiss configurations with approximately the same importance. We notice that there are more configurations in Eq. (1) that have weights significantly different from zero (including the McClure ozone configuration). This complicates the situation somewhat but does not alter the main picture of the bonding.

Reference

[1] K.P. Jensen, B.O. Roos, U. Ryde, J. Inorg. Biochem. 99 (2005) 45–54.

DOI of original article: 10.1016/j.jinorgbio.2004.11.008.
* Corresponding author. Tel.: +46 222 45 02; fax: +46 222 45 43.
E-mail address: Ulf.Ryde@teokem.lu.se (U. Ryde).

doi:10.1016/j.jinorgbio.2005.02.013